CHALMERS
UNIVERSITY OF TECHNOLOGY

Effects of Calendar and Cycle Ageing on Battery Scheduling for Optimal Energy Management: A Case Study of HSB Living Lab

Citation for the original published paper (version of record):
Mazidi, M., Khezri, R., Mohiti Ardakani, M. et al (2023). Effects of Calendar and Cycle Ageing on Battery Scheduling for Optimal Energy Management: A
Case Study of HSB Living Lab. 2023 IEEE International Conference on Energy Technologies for Future Grids. http://dx.doi.org/10.1109/ETFG55873.2023.10407383

2023 IEEE International Conference on Energy Technologies for Future Grids
Wollongong, Australia, December 3-6, 2023

Effects of Calendar and Cycle Ageing on Battery Scheduling for Optimal Energy Management: A Case Study of HSB Living Lab

Mohammadreza Mazidi, Rahmat Khezri, Maryam Mohiti, Le Anh Tuan, and David Steen
Department of Electrical Engineering
Chalmers University of Technology
Gothenburg, Sweden
{mazadi, rahmatollah.khezri, maryamar, tuan.le, david.steen}@chalmers.se

***Abstract*— This paper deals with the optimal scheduling of a building microgrid coupled with solar photovoltaic and battery energy storage (BES) considering battery degradation. The aim is to minimize the operation cost of the microgrid which includes the cost of imported electricity from the grid, the degradation cost of the battery, the cost for the peak power drawn from the grid, and the revenue from selling electricity to the grid. The nonlinear models of calendar and cycle ageing are linearized to solve the optimal scheduling as a mixed-integer linear programming (MILP) problem. The developed model is examined for a real residential building microgrid (HSB Living Lab) in Gothenburg, Sweden. The results show that if the degradation of the BES is ignored, the operation cost of the microgrid will increase by 1,394 SEK per year, and the ageing cost of the BES will also rise by 42.27%.**

Keywords*— Battery energy storage, calendar and cycle ageing, energy management, operation cost, solar PV

I. INTRODUCTION

The growing interest in renewable energy sources (RESs) has prompted the utilization of energy storages in power systems. Energy storages can facilitate the penetration of RESs by reducing the effect of uncertainty in their intermittent generation. Thus, energy storages, specifically battery energy storages (BESs), are becoming a key component in bulk systems and microgrids (MGs). Beside their role in compensating RESs' generation uncertainty, BESs can offer different services such as increasing self-consumption, energy arbitrage, and peak shaving in MGs [1]. Accordingly, with applying energy management systems (EMSs) in building microgrids, the MG owner can utilize the full potential of BESs and reduce its energy cost.

The rechargeable chemical materials of BESs, makes them degradable during cycling and storage conditions. This degradation can be accelerated by extreme charge/discharge cycles over charging/discharging and extreme low/high ambient temperature. Therefore, the precision of the BES degradation model utilized in the EMS can significantly impact the reliability of the optimal results. Aging of BES is commonly categorized into two main types: calendar aging and cycling aging [2]. Calendar ageing comprises of aging processes when the battery is idle and is independent of the charge/discharge cycle. In lithium-ion (Li-ion) BESs the calendar ageing is accelerated by increase in battery state of charge (SOC) and temperature. Cycling aging takes place during the charge and discharge cycles, with the degradation mechanism becoming more pronounced at elevated charge and discharge rates.

In many previous studies [3, 4] EMSs for BESs-integrated microgrids have been developed. However, the battery degradation is not considered. In some studies [5] that the BES degradation cost is considered the cycle ageing is only considered by imposing a penalty in the objective function. While others consider the impact of SOC or simply limit the number of cycles [6, 7]. The authors of [8] consider the battery degradation with weighted number of cycles which also incorporates the effect of SOC. In [9] the BES degradation is a convex function of charge/discharge power while the model considered in [10] links degradation to depth of discharge (DOD) similar to [11]. A neural network-based BES degradation model is incorporated for MG scheduling in [7], although historical data of the BES will be required to train the neural network. Unlike the above studies which neglect the calendar aging of the BES, few studies as [12, 13] consider both calendar and cycle aging. In [12] both ageing are modeled with a loss of capacity. However, neither DOD nor SOC is not considered in the cycle aging. Authors of [13] present a measurement-based model of the BES which calendar and cycle ageing is taken into account. Although, the calendar ageing is linked only to charge/discharge power and does not consider temperature and battery age.

This paper presents an optimal energy management of a microgrid in which the calendar and cycle ageing of the BES are incorporated. The adopted degradation models consider all major degradation factors. The nonlinear ageing terms are linearized by the method adopted from [14] making the scheduling problem a mixed-integer linear programming (MILP). In summary, the main contributions of this paper include the following:

- Development of a building microgrid energy management system with precise modelling for the calendar and cycle ageing of the battery.

The research presented in this paper received financial backing from the following sources: i) The I-GReta project, funded by the European Union's Horizon 2020 Research and Innovation program, under grant agreements No. 646039 and 775970. ii) The V2X-MAS project, supported by the Swedish Energy Agency, with project number 51811-1. iii) The FLEXIGRID project, which received funding from the European Community's Horizon 2020 Framework Programme, under grant agreement No. 864048.

978-1-6654-7164-0/23/$31.00 ©2023

- Linearizing the nonlinear terms of the BES degradation model through a generic method making it applicable to other nonlinear degradation models.
- Validating the proposed model on a real residential building MG (HSB Living Lab) located at Gothenburg, Sweden and evaluating the effects of the ageing models on the optimal results.

The subsequent sections of this paper are structured as follows: Section II elucidates the operational model of the MG. Section III outlines the BES degradation model. Section IV provides test results from the HSB real demonstration site. The conclusion is in Section V.

II. Operation Model of the MG

The envisaged optimal scheduling model is seamlessly integrated into a BMS employed within a building microgrid featuring both solar PV and BES systems. The formulation of the objective function and associated constraints is delineated as follows:

A. Objective Function

The scheduling model of the microgrid seeks to minimize the total operation cost of electricity given by:

$$f = \min_{\Xi} C^{MG} \tag{1}$$

$$C^{MG} = \sum_{d=1}^{D} \left(C_d^{im} + C_d^{peak} + C_d^{deg} - r_d^{ex}\right) \tag{2}$$

where C^{im} is the cost of imported electricity from the grid, C^{deg} is the degradation cost of battery, C^{peak} is the expense associated with the maximum power drawn from the grid. Likewise, r^{ex} is the revenue for exporting electricity to the grid by the PV and BES.

The cost of imported electricity from the grid, is calculated by multiplying the imported power ($P_{d,h}^{im}$) by the sum of fixed grid utilization cost (i.e., grid charge for electricity transmission Π^{gu}) and retail price of electricity which is assumed as the dynamic spot electricity price ($\Pi_{d,h}^{rt}$).

$$C_d^{im} = \sum_{h=1}^{H} \left(\left(\Pi_{d,h}^{rt} + \Pi^{gu}\right).P_{d,h}^{im}\right) + \Pi_d^{fix} \tag{3}$$

The cost for the peak power drawn from the grid is computed daily from the start day of optimization d to the last day of optimization D. It is calculated based on the peak demand of building until day d ($P_d^{im,\max}$) multiplied by charge for peak power (Π_d^{peak}) over the number of days in month M.

$$C_d^{peak} = \sum_{d=1}^{\mathcal{D}} \frac{\Pi_d^{peak}}{M}.P_d^{im,\max} \tag{4}$$

The total degradation cost of battery is calculated based on calendar ageing ($\psi_{d,h}^{x}$) and cycle ageing ($\psi_{d,h}^{y}$), during the optimization horizon, multiplied by the present value of the BES (Π^{BES}).

$$C_d^{deg} = \sum_{h=1}^{H} \left(\Pi^{BES}.\left(\psi_{d,h}^{x} + \psi_{d,h}^{y}\right)\right) \tag{5}$$

The revenue for exporting electricity to the grid is formulated based on the exported power to the grid ($P_{d,h}^{ex}$) multiplied by the dynamic spot electricity price plus the fixed reimbursement rate paid by the distribution network to reduce network losses (Π^{dist}).

$$r_d^{ex} = \sum_{h=1}^{H} \left(\left(\Pi_{d,h}^{rt} + \Pi^{gu}\right).P_{d,h}^{ex}\right) + \Pi_d^{fix} \tag{6}$$

B. Constraints

1) Power Balance and Grid Constraints

The power balance constraint ensures a fully power supply for the building in all time intervals. This constraint results in the balance of generation and consumption. In the generation side, there is the power generated by PV (P_t^{PV}), the discharging power of BES (P_t^{ds}), and the import power from the grid (P_t^{im}). In the consumption side, there is the building load (P_t^{Load}), the charging power of the BES (P_t^{ch}), and the exported power to the grid (P_t^{ex}).

$$P_{d,h}^{ds} + P_{d,h}^{PV} + P_{d,h}^{im} = P_{d,h}^{ch} + P_{d,h}^{Load} + P_{d,h}^{ex} \tag{7}$$

The import and export power of the grid should be less than a maximum power ($P^{g,max}$) at all time intervals. On the other hand, the MG cannot export and import to/from the grid simultaneously. Hence, binary variable u_t^g is added in equations (8) and (9) to avoid this condition.

$$0 \le P_{d,h}^{im} \le P^{g,max}.u_{d,h}^{g} \tag{8}$$

$$0 \le P_{d,h}^{ex} \le P^{g,max}.\left(1 - u_{d,h}^{g}\right) \tag{9}$$

The inverter power limitation should be considered for the PV generation plus the BES discharging power minus charging power of the BES:

$$\left|P_{d,h}^{ds} + P_{d,h}^{PV} - P_{d,h}^{ch}\right| \le P^{inv} \tag{10}$$

It is notable that extra power beyond this constraint is curtailed by the inverter.

2) BES Constraints

The constraints associated with BES modelling are as follows:

$$P_{d,h}^{ch} \in \{0\} \cup [P^{\min}, P^{\max}] \tag{11}$$

$$P_{d,h}^{ds} \in \{0\} \cup [P^{\min}, P^{\max}] \tag{12}$$

$$u_{d,h}^{ch}.P^{\min} \le P_{d,h}^{ch} \le u_{d,h}^{ch}.P^{\max} \tag{13}$$

$$u_{d,h}^{ds}.P^{\min} \le P_{d,h}^{ds} \le u_{d,h}^{ds}.P^{\max} \tag{14}$$

$$u_{d,h}^{ch} + u_{d,h}^{ds} \le 1 \tag{15}$$

$$\mathcal{O}_{d,h}^{BES} = \mathcal{O}_{d,h-1}^{BES} + \eta^{ch}\frac{P_{d,h}^{ch}.\Delta t}{E^{BES}} - \frac{P_{d,h}^{ds}.\Delta t}{\eta^{ds}.E^{BES}} \quad (16)$$

$$\mathcal{O}^{BES,\min} \le \mathcal{O}_{d,h}^{BES} \le \mathcal{O}^{BES,\max} \quad (17)$$

Constraints (11) and (12) show that the charging and discharging power of BES is either zero or varies between minimum and maximum limits, $P^{\min}$ and $P^{\max}$, respectively. Binary variables $u_{d,h}^{ch}$ and $u_{d,h}^{ds}$ are added to stop simultaneous charging and discharging. The sum of these binary variables should be equal or less than one at all time intervals. The SOC of the BES, $\mathcal{O}_{d,h}^{BES}$, changes according to the afore SOC, and energy change of battery, based on power and efficiency (η^{ch} and η^{ds}) over the battery's capacity (E^{BES}). The SOC should vary within minimum and maximum ranges ($\mathcal{O}^{BES,\min}$ and $\mathcal{O}^{BES,\max}$).

III. Battery Degradation Model

The battery degradation model is adopted from [15] where the calendar and cycle ageings are experimentally extracted for a Lithium ferro-phosphate (LFP)/graphite battery cell, that empirical calendar and cycling ageing models are also derived.

A. Calendar Ageing Model

In the extracted model by Sarasketa-Zabala et. al [16], temperature, SOC, and battery age are included in the calendar ageing. Hence, the calendar ageing model is formulated as follows:

$$\psi_{d,h}^{x} = \gamma_1 e^{\mu_1 \left(T_{d,h}^{BES}\right)^{-1}} \gamma_2 e^{\mu_2 \mathcal{O}_{d,h}^{BES}} t^{0.5} \quad (18)$$

where γ_1, γ_2, μ_1, and μ_2 are the coefficients of the extracted model. $T_{d,h}^{BES}$ represents the temperature of the battery cell during the operation and t represents the age of the battery.

B. Cycle Ageing Model

For cycle ageing, the DOD, Ah-throughput, and C-rate of the battery are included in the extracted model by Sarasketa-Zabala et. al [16]. On the other hand, the empirical model for cycle ageing is formulated for two intervals of DOD deviations. If the DOD of battery is in the range of 10%-50%, then the cycle ageing model is:

$$\psi_{d,h}^{y} = \left(\delta_1 \mathcal{D}_{d,h}^{BES^2} + \delta_2 \mathcal{D}_{d,h}^{BES} + \delta_3\right) \mathcal{K}\left(Ah_{d,h}^{BES}\right)^{0.87} \quad (19)$$

where δ_1, δ_2, and δ_3 are the coefficients. $\mathcal{D}_{d,h}^{BES}$ represents the DOD of the battery, $Ah_{d,h}^{BES}$ is the Ah-throughput of the battery, and $\mathcal{K}$ is a complex balancing factor. For DODs higher than 50% and lower than 10%, the cycle ageing model is as follows:

$$\psi_{d,h}^{y} = \left(\gamma_3 e^{\mu_3 \mathcal{D}_{d,h}^{BES}} + \gamma_4 e^{\mu_4 \mathcal{D}_{d,h}^{BES}}\right) \mathcal{K}\left(Ah_{d,h}^{BES}\right)^{0.65} \quad (20)$$

where γ_3, γ_4, μ_3, and μ_4 are the coefficients of the model.

C. Linearization of the Ageing Model

As shown by (18)–(20), the extracted models for calendar ageing and cycle ageing are nonlinear. The linear expression of the aging model can be derived using the lemmas presented in [14] as follows:

$$\sum_{i=1}^{I}\sum_{j=1}^{J} \alpha_{i,j,d,h} = 1 \quad (21)$$

$$\mathcal{O}_{d,h}^{BES} = \sum_{i=1}^{I}\sum_{j=1}^{J} \alpha_{i,j,d,h}.\hat{\mathcal{O}}_{d,h,i}^{BES} \quad (22)$$

$$Ah_{d,h}^{BES} = \sum_{i=1}^{I}\sum_{j=1}^{J} \alpha_{i,j,d,h}.\widehat{Ah}_{d,h,j}^{BES} \quad (23)$$

$$\sum_{i=1}^{I-1}\sum_{j=1}^{J-1}\left(\beta_{i,j,d,h}^{u} + \beta_{i,j,d,h}^{l}\right) = 1 \quad (24)$$

$$\begin{aligned}\alpha_{i,j,d,h} \le\ & \beta_{i,j,d,h}^{u} + \beta_{i,j,d,h}^{l} + \beta_{i,j-1,d,h}^{u} \\ & + \beta_{i-1,j-1,d,h}^{l} + \beta_{i-1,j-1,d,h}^{u} \\ & + \beta_{i-1,j,d,h}^{l}\end{aligned} \quad (25)$$

$$\psi_{d,h}^{x} = \sum_{i=1}^{I}\sum_{j=1}^{J} \alpha_{i,j,d,h}.\left(\gamma_1 e^{\mu_1 \left(T_{d,h}^{BES}\right)^{-1}} \gamma_2 e^{\mu_2 \hat{\mathcal{O}}_{d,h,i}^{BES}} t^{0.5}\right) \quad (26)$$

$$\begin{aligned}\psi_{d,h}^{y} = \sum_{i=1}^{I}\sum_{j=1}^{J} \alpha_{i,j,d,h}.\Big(&\left(\delta_1 \hat{\mathcal{D}}_{d,h,i}^{BES^2} + \delta_2 \hat{\mathcal{D}}_{d,h.i}^{BES}\right. \\ &\left. + \delta_3\right) \mathcal{K}\left(\widehat{Ah}_{d,h,j}^{BES}\right)^{0.87}\Big)\end{aligned} \quad (27)$$

$$\psi_{d,h}^{y} = \sum_{i=1}^{I}\sum_{j=1}^{J} \alpha_{i,j,d,h}.\left(\begin{array}{c}\left(\gamma_3 e^{\mu_3 \hat{\mathcal{D}}_{d,h.i}^{BES}} + \gamma_4 e^{\mu_4 \hat{\mathcal{D}}_{d,h.i}^{BES}}\right) \\ \mathcal{K}\left(\widehat{Ah}_{d,h,j}^{BES}\right)^{0.65}\end{array}\right) \quad (28)$$

where, $\alpha_{i,j,d,h} \in [0,1]$ is a continuous variable and $\beta_{i,j,d,h}^{u}$ and $\beta_{i,j,d,h}^{u}$ are binary variables with $\beta_{0,j,d,h}^{*} = \beta_{*,0,d,h}^{*} = \beta_{I,*,d,h}^{*} = \beta_{*,J,d,h}^{*} = 0$. Also, $\hat{\mathcal{O}}_{d,h,i}^{BES}$ and $\widehat{Ah}_{d,h,j}^{BES}$ are parameters associated with consecutive breakpoints in intervals of $[\ \hat{\mathcal{O}}_{d,h,1}^{BES}, \dots, \hat{\mathcal{O}}_{d,h,i}^{BES}, \hat{\mathcal{O}}_{d,h,i+1}^{BES}, \dots, \hat{\mathcal{O}}_{d,h,I}^{BES}\ ]$ and $[\widehat{Ah}_{d,h,1}^{BES}, \dots, \widehat{Ah}_{d,h,j}^{BES}, \widehat{Ah}_{d,h,j+1}^{BES}, \dots, \widehat{Ah}_{d,h,J}^{BES}]$, respectively.

IV. Simulation Results

A. Data

The developed model is assessed using a practical scenario of a residential building microgrid known as the HSB Living Lab in Gothenburg, Sweden. This facility comprises four floors and accommodates 29 apartments at present [17]. As can be seen in Fig. 1, the HSB living lab can imoprt power from the grid, PV, and BES whose characteristics are given in Table I. The load demand and the PV production at the HSB Living Lab over a one-year-period are shown in Fig. 2, which are based on historical measurements. Likewise, the price data are extracted from [18] and given in Table I. Nordpool day-ahead spot market prices are considered for the energy cost with an additional markup and taxes [19]. The values of I and J are assumed as 5 and 10, respectively. It should be noted that as the values of I and J increase, the accuracy of the results improves; however,

the running time also increases. Based on the simulations, setting the values of 5 and 10 for I and J, respectively, leads to errors of less than 10e-3 while maintaining an acceptable running time.

The EMS is solved on a daily basis for a duration of one year, aiming to ascertain the most favorable schedule for the BES and the power exchanged with the grid. The devised EMS is structured as a MILP problem, implemented through the Python programming language and executed utilizing Pyomo. The computations are performed on a personal computer equipped with a 2.90-GHz Intel Core i7 CPU and 32GB of RAM memory.

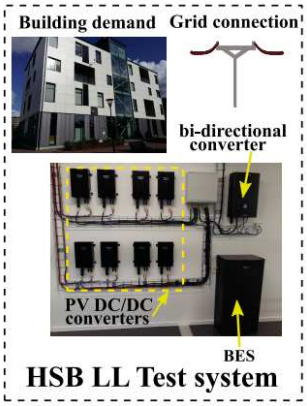

Fig. 1. Schematic of power flow in the HSB living lab [17]

TABLE I. CHARACTERISTICS OF THE SYSTEM

Characteristic	Value
PV size	18 kW
Cost of grid utilization	0.113 SEK/kWh
Charge for peak power	49.3 SEK/kWh/month
Fixed cost	20.16 SEK/day
Inverter power limit	50 kW
Battery capacity	7.2 kWh
Charger's power limits	$P^{min} = 0.5$ kW, $P^{max} = 7$ kW
SOC limit of BES	$\mathcal{O}^{BES,\min}$=10%, $\mathcal{O}^{BES,\max}$=90%
Charge/discharge efficiency	$\eta^{ch} = \eta^{ds} = 93\%$
Replacement cost of BES	11167 SEK/kWh
Maintenance cost of BES	223 SEK/year
Lifetime of BES	10 years

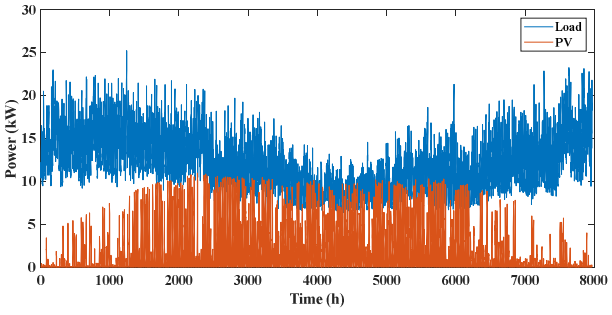

Fig. 2. Load and PV power profiles of HSB living lab

B. Case studies

Fig. 1 shows the effect of considering calendar and cycle ageing on the charging and discharging behavior of BES in a summer week. It is evident that by considering calendar ageing, the EMS prevents the BES from remaining fully charged for extended periods of time. Likewise, the inclusion of cycle ageing results in a decrease in both charging and discharging power. By considering both calendar ageing and cycle ageing, the average charging and discharging power, as well as SOC, are reduced to compensate additional ageing costs of the BES.

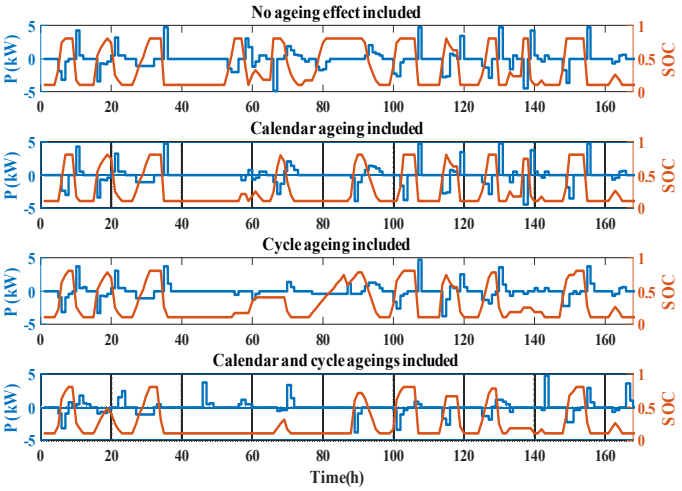

Fig. 3. The effect of calendar and cycle ageing on the charging and discharging behavior of BES

The economic results of the system for one year have been compared with and without considering ageing of BES in Table II. The results show that when the aging of the BES is not considered, although the import cost decrease and export revenue increases, the total cost of the system increases by 1394.24 SEK which is due to the higher ageing level of the BES. On the other hand, total ageing cost of the BES increases by 42.27%, resulting in a significant reduction in the lifetime of the BES. Therefore, it is essential to consider the ageing of the BES in the EMS.

The effects of accounting for degradation costs on the ageing of BES are investigated in Table III. As can be seen, total degradation of the BES is 7.07%, with both cycle ageing and calendar ageing contributing almost equally to this figure. However, when degradation costs are not taken into account, the total degradation increases to 10.07%, resulting in an additional cost of 3% which mainly comes from the cycle ageing of the BES.

TABLE II. YEARLY ECONOMIC RESULTS OF THE SYSTEM

Model	Total cost (SEK)	Import cost (SEK)	Export rev. (SEK)	Cyc. age. cost (SEK)	Cal. age. cost (SEK)
With degrad.	171,206	165,737	221.86	3,205	2,485
w/o degrad.	172,600.83	164,858.37	354.61	5,045.24	3,051.83

TABLE III. EFFECT OF CONSIDERING DEGRADATION COST ON AGEING OF BES

Model	Total deg. (%)	Cyc. age. (%)	Cal. age. (%)
With Cyc. Age and Cal. Age	7.0783	3.9866	3.0917
w/o degrad.	10.0707	6.2750	3.7957

The cost associated with cycle ageing and calendar ageing is directly influenced by the accuracy of their parameters, which are estimated using practical experiments. Figure 4 investigates the sensitivity of the system cost concerning the estimation error in parameters of cycle ageing and calendar ageing. It is assumed that the estimation error results in an increase in the value of ageing. As expected, the system cost increases with an increase in the estimation error. However, it is observed that cycle ageing is more sensitive to the estimation error compared to calendar ageing. This result highlights the need for accurate and reliable experiment for estimating parameters in the cycle ageing model.

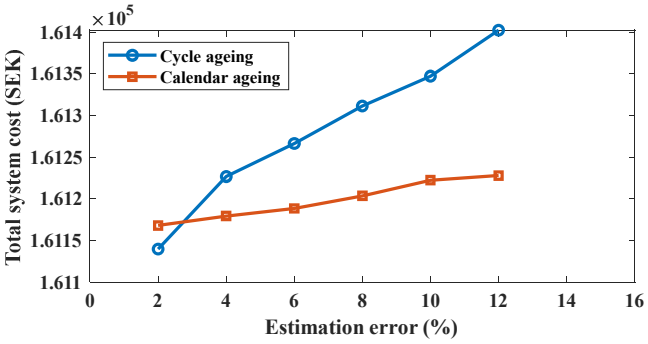

Fig. 4. Sensitivity of the system cost with respect to the estimation error in parameters of cycle ageing and calendar ageing

V. CONCLUSION

his article introduces an EMS tailored for building microgrids, encompassing comprehensive degradation models accounting for both calendar and cycling aging of BESs. To gauge the efficacy of the proposed EMS, real-world case studies were conducted. These studies were built upon data acquired from the HSB Living Lab, situated on the premises of Chalmers University of Technology. Our first step was to demonstrate the impact of incorporating calendar and cycle ageing costs of BES into the optimization model. The results indicated that, without including the degradation into the optimization model, the total system cost was increased by 1394 SEK, and the ageing costs of the BES was increased by 42.27% compared to a model that considered degradation. Secondly, we investigated the sensitivity of the system cost to the estimation error in parameters of cycle ageing and calendar ageing. Our findings revealed that cycle ageing is more sensitive to estimation errors when compared to calendar ageing. Therefore, it is of utmost importance to precisely estimate its parameters.

REFERENCES

[1] R. Khezri, A. Mahmoudi, and H. Aki, "Optimal planning of solar photovoltaic and battery storage systems for grid-connected residential sector: Review, challenges and new perspectives," *Renewable Sustain. Energy Rev.*, vol. 153, Jan. 2022.

[2] E. Redondo-Iglesias, P. Venet, and S. Pelissier, "Calendar and cycling ageing combination of batteries in electric vehicles, " *Microelectron. Rel.*, vols. 88–90, pp. 1212–1215, Sep. 2018.

[3] A. Merabet, K. T. Ahmed, H. Ibrahim, R. Beguenane, and A. Y. M. Ghias, "Energy management and control system for laboratory scale microgrid based wind-PV-battery, " *IEEE Trans. Sustain. Energy*, vol. 8, no. 1, pp. 145–154, Jan. 2017.

[4] K. Thirugnanam, S. K. Kerk, C. Yuen, N. Liu, and M. Zhang, "Energy management for renewable microgrid in reducing diesel generators usage with multiple types of battery," *IEEE Trans. Ind. Electron.*, vol. 65, no. 8, pp. 6772–6786, Aug. 2018.

[5] B. Li, T. Chen, X. Wang, and G. B. Giannakis, "Real-time energy management in microgrids with reduced battery capacity requirements," *IEEE Trans. Smart Grid*, vol. 10, no. 2, pp. 1928–1938, Mar. 2019.

[6] J. A. Pinzon, P. P. Vergara, L. C. Da Silva, and M. J. Rider, "Optimal management of energy consumption and comfort for smart buildings operating in a microgrid, " *IEEE Trans. Smart Grid*, vol. 10, no. 3, pp. 3236-3247, 2018.

[7] Cunzhi Zhao and Xingpeng Li, "Microgrid Optimal Energy Scheduling Considering Neural Network based Battery Degradation", *IEEE Trans. Power Sys.*, early access, Jan. 2023.

[8] M. Alramlawi and P. Li, "Design optimization of a residential PV-battery microgrid with a detailed battery lifetime estimation model," *IEEE Trans. Ind. Appl.*, vol. 56, no. 2, pp. 2020–2030, 2020.

[9] J. E. Contreras-Ocana, M. A. Ortega-Vazquez, and B. Zhang, "Participation of an energy storage aggregator in electricity markets, " *IEEE Trans. Smart Grid*, vol. 10, no. 2, pp. 1171-1183, 2017.

[10] M. Koller, T. Borsche, A. Ulbig, and G. Andersson, "Defining a degradation cost function for optimal control of a battery energy storage system," in *Proc. IEEE Grenoble Powertech Conf.*, Grenoble, France, 2013, pp. 1–6.

[11] C. Ju, P. Wang, L. Goel, and Y. Xu, "A two-layer energy management system for microgrids with hybrid energy storage considering degradation costs, " *IEEE Trans. Smart Grid*, vol. 9, no. 6, pp. 6047-6057, 2017.

[12] G. Cardoso, T. Brouhard, N. DeForest, D. Wang, M. Heleno, and L. Kotzur, "Battery aging in multi-energy microgrid design using mixed integer linear programming, " *Appl. Energy*, vol. 231, pp. 1059-1069, 2018.

[13] K. Antoniadou-Plytaria, D. Steen, O. Carlson, and M. A. F. Ghazvini, "Market-based energy management model of a building microgrid considering battery degradation, " *IEEE Trans. Smart Grid*, vol. 12, no. 2, pp. 1794-1804, 2020.

[14] M. Mohiti, M. Mazidi, N. Rezaei, and M.-H. Khooban, "Role of vanadium redox flow batteries in the energy management system of isolated microgrids, " *J. Energy Storage*, vol. 40, p. 102673, 2021.

[15] E. Sarasketa-Zabala, E. Martinez-Laserna, M. Berecibar, I. Gandiaga, L. M. Rodriguez-Martinez, and I. Villarreal, "Realistic lifetime prediction approach for Li-ion batteries, " *Appl. Energy*, vol. 162, pp. 839-852, 2016.

[16] E. Sarasketa-Zabala, I. Gandiaga, E. Martinez-Laserna, L. M. RodriguezMartinez, and I. Villarreal, "Cycle ageing analysis of a lifepo4/graphite cell with dynamic model validations: Towards realistic lifetime predictions," *J. Power Sources*, vol. 275, pp. 573–587, 2015.

[17] H. L. L. Chalmers University of Technology, " 2023. [Online]. Available: https://hll.livinglab.chalmers.se/.

[18] Gothenburge Energy, " 2023. [Online]. Available: https://www.goteborgenergi.se/english.

[19] Nord Pool, " 2023. [Online]. Available: https://www.nordpoolgroup.com/Marketdata1/Intraday/Market-data1/Marketdata1/Overview/?view=table.